Supporting Information

Oriented Nanosheet-Assembled CoNi-LDH Cages with Efficient Ion Diffusion for Quasi-Solid-State Hybrid Supercapacitors

Zixiao Li,[a] Hongyu Mi,*[a] Fengjiao Guo,[a] Chenchen Ji,*[a] Shixue He,[a] Han Li,[a] and Jieshan Qiu*[b]

[a]*School of Chemical Engineering and Technology, Xinjiang University, Urumqi 830046, Xinjiang, China*

[b]*State Key Laboratory of Chemical Resource Engineering, College of Chemical Engineering, Beijing University of Chemical Technology, Beijing 100029, China*

EXPERIMENTAL SECTION

Preparation of ZIF-67 and derived CoNi-LDH$_x$. ZIF-67 was first produced using the method presented previously.[1] Then, CoNi-LDH$_x$ was prepared based on the ion-exchange reaction between ZIF-67 and $Ni(NO_3)_2 \cdot 6H_2O$. Typically, the dispersion of 40 mg ZIF-67 in 20 mL ethanol was added in the solution of 80 mg $Ni(NO_3)_2 \cdot 6H_2O$ in 20 mL ethanol. After the above mixture was refluxed for 2 h at 90 °C, the solid (CoNi-LDH$_2$) was acquired by filtering, washing with ethanol, and drying at 60 °C. Similarly, the comparative samples named as CoNi-LDH$_1$ and CoNi-LDH$_3$ were prepared by altering the mass ratio of ZIF-67 and Ni salt (1:1 and 1:3), respectively.

Materials Characterization. Scanning electron microscopy (SEM, SU-8010) was employed to study the morphologies of various products. Their microstructures were made clear by employing atomic force microscopy (AFM, Brüker Dimension Icon) and transmission electron microscopy (TEM, 2100F). The phase feature was verified via X-ray diffraction (XRD, Brüker D8 advance), and the elemental components were clarified by X-ray photoelectron spectroscopy (XPS, Thermo Fisher ESCALAB 250Xi). Nitrogen adsorption-desorption apparatus (ASAP 2460) was employed for the surface area and pore structure. The water contact angle was tested by the DCAT21 equipment.

Electrochemical Characterizations. Electrochemical properties were studied on the CHI660b workstation and CT2001A battery tester. First, various samples were made into the electrodes through pressing the sheet containing active materials, acetylene black, and polytetrafluoroethylene (mass ratio of 8:1:1) on the Ni surface (about 2.5 mg cm^{-2} for active material). Then, these electrodes were built into a three-electrode system with Pt (counter electrode) and Hg/HgO (reference electrodes), employing 2 M KOH electrolyte. Gravimetric capacities (Q_g, C g^{-1}) were gained from equation S1:[2]

$$Q_g = \frac{2I\int V\mathrm{d}t}{mV} \quad \text{(S1)}$$

where I, $\int V\mathrm{d}t$, m, and V belong to the discharge current (A), integral area under a discharge curve (V s), mass of active material, (g) and potential window (V), respectively. Both aqueous and quasi-solid-state HSCs used CoNi-LDH_2 positive electrode and AC negative electrode, where the former employed the glass microfiber separator and 2 M KOH electrolyte, whereas the latter used the PVA/KOH gel electrolyte/separator. In order to obtain PVA/KOH, PVA (1 g) and KOH (1 g) were added in deionized water (10 mL) and heated at 85 °C under vigorous stirring, followed by curing this gel at room temperature.[3] In HSCs, the mass ratio for CoNi-LDH_2 and AC was calculated according to equation S2:[4–6]

$$\frac{m_+}{m_-} = \frac{Q_{g-}}{Q_{g+}} \quad \text{(S2)}$$

where m is the mass of active electrode material (g) and Q is the gravimetric capacity (C g^{-1}).[4–6] The optimized ratio is 1:3.4, and the total active mass in the device is about 4.4 mg. The gravimetric capacity (Q_{cell}, C g^{-1}), energy density (E, Wh kg^{-1}), and power density (P, W kg^{-1}) were decided by equations S3, S4, and S5:[7–10]

$$Q_{cell} = \frac{2I\int V\mathrm{d}t}{MV} \quad \text{(S3)}$$

$$E = \frac{I\int V\mathrm{d}t}{3.6M} \quad \text{(S4)}$$

$$P = \frac{3600E}{t} \quad \text{(S5)}$$

where V, M, and t correspond to the voltage window (V), total mass of active materials for the device (g), and discharge time (s), respectively.[7–10]

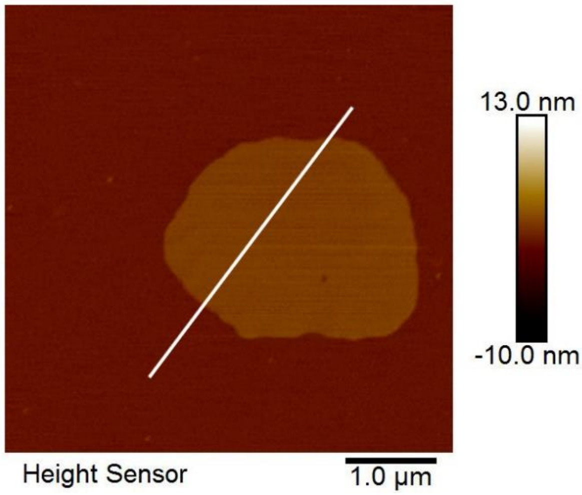

Figure S1. AFM image of CoNi-LDH$_2$.

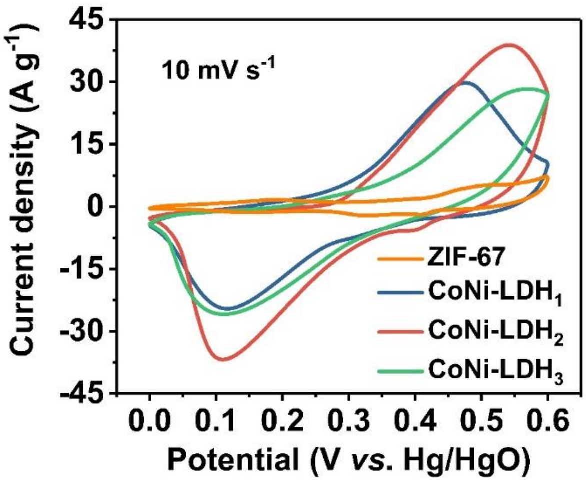

Figure S2. CV profiles of ZIF-67, CoNi-LDH$_1$, CoNi-LDH$_2$, and CoNi-LDH$_3$ electrodes at a sweep rate of 10 mV s^{-1}.

Table S1. Performance comparison of $CoNi\text{-}LDH_2$ with other materials.

Electrode material	Electrolyte	Capacity (capacitance) at a low sweep rate	Retention	Ref.
NiCo-LDH@NCF	2 M KOH	756C g^{-1} (0.5 A g^{-1})	54.8% (20 A g^{-1})	11
MnO_2@NiCo-LDH/CoS_2	2 M KOH	1547 F g^{-1} (1 A g^{-1})	76.9% (10 A g^{-1})	12
CC@$NiCo_2$Al-LDH	1 M KOH	1137 F g^{-1} (0.5 A g^{-1})	58% (20 A g^{-1})	13
CoS_x/Ni-Co LDH	2 M KOH	1562 F g^{-1} (1 A g^{-1})	65.4% (20 A g^{-1})	14
Co-Ni-B-S	6 M KOH	1281 F g^{-1} (1 A g^{-1})	62.7% (20 A g^{-1})	15
NiCo-LDH/PANI/BC	2 M KOH	761 C g^{-1} (1 A g^{-1})	46% (15 A g^{-1})	16
Co(II)-TMU-63#30%$CoMn_2O_4$ NCP	2 M KOH	1420 F g^{-1} (7 A g^{-1})	32.4% (18 A g^{-1})	17
PNT@NiCo-LDH	6 M KOH	1448.2 F g^{-1} (1 A g^{-1})	44.8% (20 A g^{-1})	18
NCLP@NiMn-LDH	6 M KOH	2318 F g^{-1} (1 A g^{-1})	60% (20 A g^{-1})	19
OCS/NiCo-LDH@Ni foam	3 M KOH	1784 F g^{-1} (1 A g^{-1})	41% (10 A g^{-1})	20
NiCo-LDHs FMs	6 M KOH	622 C g^{-1} (1 A g^{-1})	56.7% (10 A g^{-1})	21
Mn–Co LDH@CDs	1 M LiOH	2063 F g^{-1} (1 A g^{-1})	43.8% (10 A g^{-1})	22
NiMn-LDH (Ov-LDH)	2 M KOH	1183 C g^{-1} (1 A g^{-1})	63.8% (30 A g^{-1})	23
$CoNi\text{-}LDH_2$	**2 M KOH**	**1031.4 C g^{-1} (2062.4 F g^{-1}) (1 A g^{-1})**	**64.7% (25 A g^{-1})**	**This work**

REFERENCES

(1) Hu, H.; Guan, B.; Xia, B.; Lou, X. W. Designed Formation of Co_3O_4/$NiCo_2O_4$ Double-Shelled Cages with Enhanced Pseudocapacitive and Electrocatalytic Properties. *J. Am. Chem. Soc.* **2015**, *137*, 5590−5595.

(2) Liang, H.; Xia, C.; Jiang, Q.; Gandi, A. N.; Schwingenschlögl, U.; Alshareef, H.

N. Low Temperature Synthesis of Ternary Metal Phosphides Using Plasma for Asymmetric Supercapacitors. *Nano Energy* **2017**, *35*, 331−340.

(3) Li, Z.; Mi, H.; Bai, Z.; Ji, C.; Sun, L.; Gao, S.; Qiu, J. Sustainable Biowaste Strategy to Fabricate Dual-Doped Carbon Frameworks with Remarkable Performance for Flexible Solid-State Supercapacitors. *J. Power Sources* **2019**, *418*, 112−121.

(4) Wulan Septiani, N. L.; Kaneti, Y. V.; Fathoni, K. B.; Wang, J.; Ide, Y.; Yuliarto, B.; Nugraha; Dipojono, H. K.; Nanjundan, A. K.; Golberg, D.; Bando, Y.; Yamauchi, Y. Self-Assembly of Nickel Phosphate-Based Nanotubes into Two-Dimensional Crumpled Sheet-Like Architectures for High-Performance Asymmetric Supercapacitors. *Nano Energy* **2020**, *67*, 104270.

(5) Sun, J.; Yu, X.; Zhao, S.; Chen, H.; Tao, K.; Han, L. Solvent-Controlled Morphology of Amino-Functionalized Bimetal Metal-Organic Frameworks for Asymmetric Supercapacitors. *Inorg. Chem.* **2020**, *59*, 11385−11395.

(6) He, S.; Li, Z.; Mi, H.; Ji, C.; Guo, F.; Zhang, X.; Li, Z.; Du, Q.; Qiu, J. 3D Nickel-Cobalt Phosphide Heterostructure for High-Performance Solid-State Hybrid Supercapacitors. *J. Power Sources* **2020**, *467*, 228324.

(7) Chen, Y.; Zhou, T.; Li, L.; Pang, W. K.; He, X.; Liu, Y. N.; Guo, Z. Interfacial Engineering of Nickel Boride/Metaborate and Its Effect on High Energy Density Asymmetric Supercapacitors. *ACS Nano* **2019**, *13*, 9376−9385.

(8) Su, L.; Gong, L.; Wang, X.; Pan, H. Improved Low-Temperature Performance of Novel Asymmetric Supercapacitor with Capacitor/Battery-Capacitor Construction. *Int. J. Energy Res.* **2016**, *40*, 763−769.

(9) Ling, Y.; Chen, H.; Zhou, J.; Tao, K.; Zhao, S.; Yu, X.; Han, L. Metal-Organosulfide Coordination Polymer Nanosheet Array as a Battery-Type Electrode for an Asymmetric Supercapacitor. *Inorg. Chem.* **2020**, *59*, 7360−7369.

(10) He, S.; Guo, F.; Yang, Q.; Mi, H.; Li, J.; Yang, N.; Qiu, J. Design and Fabrication of Hierarchical NiCoP–MOF Heterostructure with Enhanced Pseudocapacitive Properties. *Small* **2021**, *17*, 2100353.

(11) Liu, Y.; Wang, Y.; Shi, C.; Chen, Y.; Li, D.; He, Z.; Wang, C.; Guo, L.; Ma, J. Co-ZIF Derived Porous NiCo-LDH Nanosheets/N Doped Carbon Foam for High-Performance Supercapacitor. *Carbon* **2020**, *165*, 129−138.

(12) Wang, X.; Huang, F.; Rong, F.; He, P.; Que, R.; Jiang, S. P. Unique MOF-Derived Hierarchical MnO_2 Nanotubes@NiCo-LDH/CoS_2 Cage Materials as High Performance Supercapacitors. *J. Mater. Chem. A* **2019**, *7*, 12018−12028.

(13) Li, Z.; Mi, H.; Bai, Z.; Ji, C.; Sun, L.; Gao, S.; Qiu, J. Sustainable Biowaste Strategy to Fabricate Dual-Doped Carbon Frameworks with Remarkable Performance for Flexible Solid-State Supercapacitors. *J. Power Sources* **2019**, *418*, 112−121.

(14) Guan, X.; Huang, M.; Yang, L.; Wang, G.; Guan, X. Facial Design and Synthesis of CoS_x/Ni-Co LDH Cages with Rhombic Dodecahedral Structure for High-Performance Asymmetric Supercapacitors. *Chem. Eng. J.* **2019**, *372*, 151−162.

(15) Wang, Q.; Luo, Y.; Hou, R.; Zaman, S.; Qi, K.; Liu, H.; Park, H. S.; Xia, B. Y. Redox Tuning in Crystalline and Electronic Structure of Bimetal–Organic Frameworks Derived Cobalt/Nickel Boride/Sulfide for Boosted Faradaic Capacitance. *Adv. Mater.* **2019**, *31*, 1905744.

(16) Wu, H.; Zhang, Y.; Yuan, W.; Zhao, Y.; Luo, S.; Yuan, X.; Zheng, L.; Cheng, L. Highly Flexible, Foldable and Stretchable Ni-Co Layered Double Hydroxide/Polyaniline/Bacterial Cellulose Electrodes for High-Performance All-Solid-State Supercapacitors. *J. Mater. Chem. A* **2018**, *6*, 16617−16626.

(17) Abazari, R.; Sanati, S.; Morsali, A.; Dubal, D. P. High Specific Capacitance of A 3D-Metal-Organic Framework-Confined Growth in $CoMn_2O_4$ Nanostars as Advanced Supercapacitor Electrode Materials. *J. Mater. Chem. A* **2021**, *9*, 11001−11012.

(18) Zang, Y.; Luo, H.; Zhang, H.; Xue, H. Polypyrrole Nanotube-Interconnected NiCo-LDH Nanocages Derived by ZIF-67 for Supercapacitors. *ACS Appl. Energy Mater.* **2021**, *4*, 1189−1198.

(19) Liang, H.; Lin, J.; Jia, H.; Chen, S.; Qi, J.; Cao, J.; Lin, T.; Fei, W.; Feng, J. Hierarchical NiCo-LDH/NiCoP@NiMn-LDH Hybrid Electrodes on Carbon Cloth for Excellent Supercapacitors. *J. Mater. Chem. A* **2018**, *6*, 15040−15046.

(20) Wang, Q.; Wang, X.; He, H.; Chen, W. ZIF-67 Derived Hollow OCS/NiCo-LDH Nanocages as Binder-Free Electrodes for High Performance Supercapacitors. *Appl. Clay Sci.* **2020**, *198*, 105820.

(21) Chu, D.; Song, X.; Tan, L.; Ma, H.; Pang, H.; Wang, X.; Guo, D. Polyvinyl Pyrrolidone-Induced Assembly of NiCo-LDHs Nanosheets: A Facile Method for Fabricating Three-Dimensional Flower-Like Microspheres with Excellent Supercapacitor Performance. *Inorg. Chem. Commun.* **2019**, *110*, 107587.

(22) Song, L.; Peng, C.; Yang, F.; Wang, L.; Jiang, Y.; Wang, Y. Surface Spatial Confinement Effect on Mn–Co LDH@Carbon Dots for High-Performance

Supercapacitors. *ACS Appl. Energy Mater*. **2021**, *4*, 4654−4661.

(23) Tang, Y.; Shen, H.; Cheng, J.; Liang, Z.; Qu, C.; Tabassum, H.; Zou, R. Fabrication of Oxygen-Vacancy Abundant NiMn-Layered Double Hydroxides for Ultrahigh Capacity Supercapacitors. *Adv. Funct. Mater*. **2020**, *30*, 1908223.